Original Article | Neuroimaging and Head & Neck

eISSN 2005-8330
https://doi.org/10.3348/kjr.2023.0591
Korean J Radiol 2024;25(2):166-178

Korean Journal of Radiology
KJR

Combining Non-Contrast CT Signs With Onset-to-Imaging Time to Predict the Evolution of Intracerebral Hemorrhage

Lei Song[1], Xiaoming Qiu[1], Cun Zhang[2], Hang Zhou[3], Wenmin Guo[4], Yu Ye[1], Rujia Wang[5], Hui Xiong[1], Ji Zhang[6], Dongfang Tang[7], Liwei Zou[8], Longsheng Wang[8], Yongqiang Yu[9], Tingting Guo[10]

[1]Department of Radiology, Huangshi Central Hospital, Affiliated Hospital of Hubei Polytechnic University, Huangshi, China
[2]Department of Radiology, The First Affiliated Hospital of University of Science and Technology of China, Hefei, China
[3]Department of Radiology, Xiangyang Central Hospital, Affiliated Hospital of Hubei University of Arts and Science, Xiangyang, China
[4]Department of Radiology, Xiangyang No. 1 People's Hospital, Hubei University of Medicine, Xiangyang, China
[5]Department of Radiology, Tangshan Gongren Hospital, Tangshan, China
[6]Department of Clinical Laboratory, Xiangyang Central Haspital, Affiliated Hospital of Hubei University of Arts and Science, Xiangyang, China
[7]Department of Neurosurgery, Xiangyang Central Hospital, Affiliated Hospital of Hubei University of Arts and Science, Xiangyang, China
[8]Department of Radiology, The Second Affiliated Hospital of Anhui Medical University, Hefei, China
[9]Department of Radiology, The First Affiliated Hospital of Anhui Medical University, Hefei, China
[10]Department of Nuclear Medicine, Huangshi Central Hospital, Affiliated Hospital of Hubei Polytechnic University, Huangshi, China

Objective: This study aimed to determine the predictive performance of non-contrast CT (NCCT) signs for hemorrhagic growth after intracerebral hemorrhage (ICH) when stratified by onset-to-imaging time (OIT).

Materials and Methods: 1488 supratentorial ICH within 6 h of onset were consecutively recruited from six centers between January 2018 and August 2022. NCCT signs were classified according to density (hypodensities, swirl sign, black hole sign, blend sign, fluid level, and heterogeneous density) and shape (island sign, satellite sign, and irregular shape) features. Multivariable logistic regression was used to evaluate the association between NCCT signs and three types of hemorrhagic growth: hematoma expansion (HE), intraventricular hemorrhage growth (IVHG), and revised HE (RHE). The performance of the NCCT signs was evaluated using the positive predictive value (PPV) stratified by OIT.

Results: Multivariable analysis showed that hypodensities were an independent predictor of HE (adjusted odds ratio [95% confidence interval] of 7.99 [4.87–13.40]), IVHG (3.64 [2.15–6.24]), and RHE (7.90 [4.93–12.90]). Similarly, OIT (for a 1-h increase) was an independent inverse predictor of HE (0.59 [0.52–0.66]), IVHG (0.72 [0.64–0.81]), and RHE (0.61 [0.54–0.67]). Blend and island signs were independently associated with HE and RHE (10.60 [7.36–15.30] and 10.10 [7.10–14.60], respectively, for the blend sign and 2.75 [1.64–4.67] and 2.62 [1.60–4.30], respectively, for the island sign). Hypodensities demonstrated low PPVs of 0.41 (110/269) or lower for IVHG when stratified by OIT. When OIT was ≤ 2 h, the PPVs of hypodensities, blend sign, and island sign for RHE were 0.80 (215/269), 0.90 (142/157), and 0.83 (103/124), respectively.

Conclusion: Hypodensities, blend sign, and island sign were the best NCCT predictors of RHE when OIT was ≤ 2 h. NCCT signs may assist in earlier recognition of the risk of hemorrhagic growth and guide early intervention to prevent neurological deterioration resulting from hemorrhagic growth.

Keywords: Stroke; Intracerebral hemorrhage; Hemorrhagic growth; Time; Computed tomography

Received: June 29, 2023 **Revised:** November 5, 2023 **Accepted:** November 19, 2023

Corresponding author: Tingting Guo, MM, Department of Nuclear Medicine, Huangshi Central Hospital, Affiliated Hospital of Hubei Polytechnic University, No. 141, Tianjin Road, Huangshigang District, Huangshi 435000, China
• E-mail: 757608096@qq.com
Corresponding author: Yongqiang Yu, MD, PhD, Department of Radiology, The First Affiliated Hospital of Anhui Medical University, No. 218, Jixi Road, Shushan District, Hefei 230022, China
• E-mail: cjr.yuyongqiang@vip.163.com

Korean Journal of Radiology
KJR

INTRODUCTION

Intracerebral hemorrhage (ICH), which constitutes 10%–15% of all stroke-related events, accounts for approximately half of all deaths [1]. Hematoma expansion (HE) occurs in approximately 30% of patients with ICH within 6 h after symptom onset [2], is associated with deterioration [3], and is a promising therapeutic target [4]. Despite progress in curbing HE, clinical trial interventions have not significantly improved patient outcomes [5].

The conventional definition of HE emphasizes the growth of a hematoma in the brain parenchyma [6] while ignoring the dynamic changes in intraventricular hemorrhage (IVH) [4,7,8]. Notably, IVH growth (IVHG) is clinically not uncommon and has been linked to a poor prognosis [7]. Recent studies have suggested that the incorporation of IVHG into the HE definition can boost the predictive accuracy of outcomes in patients with ICH and have proposed the definition of revised HE (RHE) [9,10].

Extensive evidence supports the positive effect of non-contrast CT (NCCT) signs on HE [11,12]. Owing to some degree of overlap between NCCT signs, it is difficult to compare their predictive accuracy with regard to clinical outcome prediction [11]. Currently, few studies have conducted multivariable analyses to evaluate the hemorrhagic growth factors associated with all NCCT signs. The time from onset to the first imaging time (onset-to-imaging time [OIT]) is another factor closely associated with hemorrhagic growth after ICH [13]. A recent study indicated that the diagnostic performance of NCCT signs in predicting HE is affected by OIT. Hypodensities were identified in four out of five patients with HE within 2 h of onset, whereas irregular shapes performed better in late presenters [14]. However, they did not provide a comprehensive survey of all currently available NCCT signs. It is also unknown whether the predictive performance of NCCT signs for IVHG or RHE is limited by OIT.

To date, a comprehensive analysis investigating the association between hemorrhagic growth (HE, IVHG, and RHE) and NCCT signs while considering OIT is lacking. Therefore, the goal of this study was to examine whether the association between the above-mentioned signs and hemorrhagic growth was modified by OIT and to determine the predictive performance of NCCT signs for hemorrhagic growth when stratified by OIT.

MATERIALS AND METHODS

Patient Selection

The Institutional Review Board granted a waiver/exemption owing to the use of de-identified data (IRB No. PJ2022-09-30, 2022-22, 2021-036, XYYYE20220081, YX2023-134, and GRYY-LL-KJ2022-K820). We retrospectively included consecutive patients with spontaneous ICH who were admitted to six stroke centers between January 2018 and August 2022. The inclusion criteria were 1) supratentorial ICH, 2) individuals aged > 18 years, 3) OIT ≤ 6 h, and 4) follow-up NCCT within 48 h of initial ictus. The exclusion criteria were 1) multiple ICH hematomas, 2) primary IVH, 3) surgical hematoma evacuation before the follow-up NCCT, 4) secondary ICH ascribed to trauma, vascular malformation, moyamoya disease, aneurysm, neoplastic disease, or a hemorrhagic transformation of a cerebral infarction, 5) prior oral/intravenous anticoagulant therapy, or abnormal coagulation at admission laboratory values (international normalized ratio [INR] > 1.7, platelet count < 50 x 10^9/μL), and 6) severe NCCT imaging artifacts during examinations.

Clinical Data

Variables included demographic, laboratory, clinical, and outcome characteristics. These included age, sex, alcohol consumption, smoking, medical history (ICH, cerebral infarction, hypertension, and diabetes mellitus), admission laboratory results (glucose, platelet count, and INR), systolic blood pressure, diastolic blood pressure, and baseline Glasgow Coma Scale scores. OIT was sorted into three tertiles as previously described: ≤ 2 h, 2–4 h, and 4–6 h [15]. Neurological function was assessed through outpatient visits or telephone consultations using the modified Rankin Scale (mRS) score (dichotomized as favorable [0–2] and poor [3–6]) at 90 days [9].

Neuroimaging

NCCT images were obtained using a 5-mm slice thickness. ICH volume measurements were performed using semi-automated segmentation with 3D Slicer software (version 4.11.2; https://www.slicer.org/). Two radiologists (with 10 and 5 years of experience) independently measured the ICH volume at baseline and follow-up NCCTs. When the difference in volume measurements between the two researchers showed ≥ 1 mL, the final volume was re-assessed by both researchers through mutual discussion to reach a consensus, and the mean of both was used as

 https://doi.org/10.3348/kjr.2023.0591

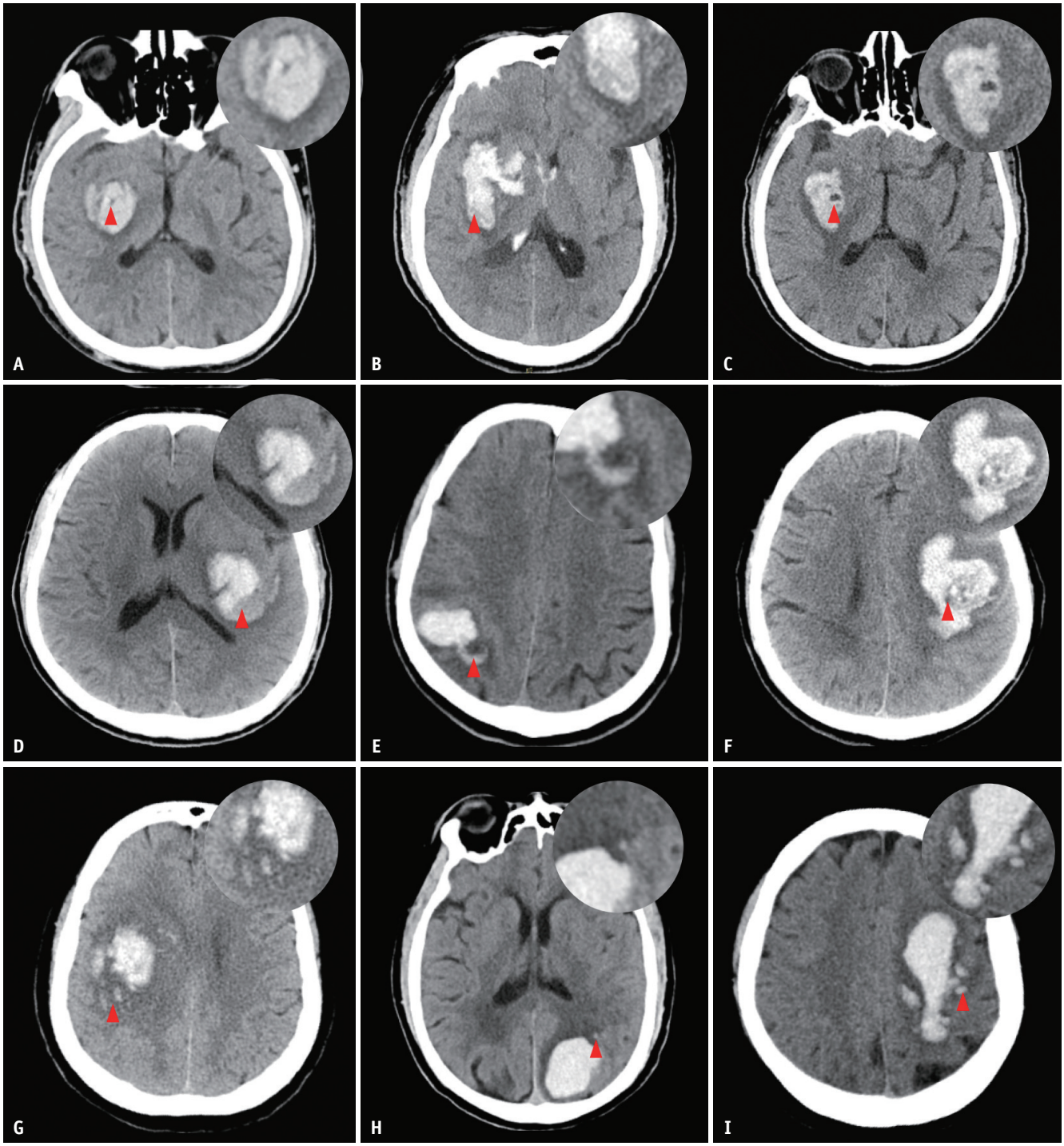

Fig. 1. Illustrative examples of signs (arrowheads). **A:** Hypodensities (any hypodense area was strictly enclosed within the hematoma, regardless of size, shape, or density). **B:** Swirl sign (rounded, streaklike, or irregular region of hypo- or isoattenuation compared with the brain parenchyma. Does not have to be encapsulated in the hematoma). **C:** Black hole sign (similar to the hypodensities but with a well-defined margin and a density difference > 28 HUs between the 2 regions). **D:** Blend sign (the difference between a relatively hypoattenuating region and a hyperattenuating area of the hematoma should be at least 18 HU, and with an identifiable border). **E:** Fluid level (there was a straight line separating the two densities within the hematoma, with hypoattenuating a region above and a hyperattenuating region below). **F:** Heterogeneous density (3 or more foci of hypoattenuation were found in the largest hematoma region, with the axial slice equivalent to a Barras density scale ≥ 3). **G:** Island sign (at least 3 scattered small hematomas all separate from the main intracerebral hemorrhage or at least 4 small hematomas some or all of which may connect with the hematoma). **H:** Satellite sign (a hematoma (diameter < 10 mm) was 1 to 20 mm away from the main hematoma). **I:** Irregular shape (there were 2 or more focal hematoma margin irregularities within the largest hematoma, with the axial slice equivalent to a Barras shape scale ≥ 3). HU = Hounsfield unit

https://doi.org/10.3348/kjr.2023.0591

Korean Journal of Radiology
KJR

a final result. Indistinguishable boundaries between the parenchymal hematoma and IVH, if present, were manually segmented by a trained radiologist (5 years of experience). ICH locations, including the basal ganglia, thalamus, and lobar region, were assigned by a stroke neurologist (10 years of experience), as previously reported [16,17].

The NCCT signs were classified into two categories based on density (hypodensities, swirl sign, black hole sign, blend sign, fluid level, and heterogeneous density) and shape (island sign, satellite sign, and irregular shape). The NCCT signs were evaluated according to the International NCCT ICH Study Group criteria (Fig. 1) [11]. An experienced radiologist and stroke neurologist (with 10 and 5 years of experience, respectively), who were blinded to the clinical and outcome information, independently reviewed the axial NCCT images. Any discordant opinions were resolved by consulting a third senior neuroradiologist (20 years of experience). Coronal and sagittal reconstructions, if necessary, were applied for differential diagnosis to discern imaging signs from the partial volume effect, particularly in terms of hypodensities and the black hole sign.

HE was defined as absolute hematoma growth > 6 mL or relative hematoma growth > 33% from the initial to follow-up NCCTs [18], whereas IVHG was defined as either absolute IVH growth > 1 mL by comparing the initial and follow-up NCCTs or any IVH on the follow-up NCCT but without the presence of IVH on the initial NCCT [7,9]. RHE was classified into four types as follows: HE > 6 mL, relative hematoma growth > 33%, IVHG > 1 mL, or any IVH on follow-up NCCT [10].

Statistical Analysis

Due to the retrospective nature of this study, sample size calculations were not performed. Quantitative data were evaluated for normality (Kolmogorov-Smirnov test) and equal variance (Levene's test) before further analysis. Normally and non-normally distributed data were expressed as mean (standard deviation) or median (interquartile range [IQR]), respectively. Categorical data are presented as counts and percentages. The inter-reader agreement between different measurements of ICH volume was assessed using the Bland-Altman analysis. The agreement on each NCCT sign was evaluated using Cohen's kappa coefficient (κ). Baseline characteristics are summarized separately for NCCT signs and presented separately for those with and without signs.

The Chi-squared (χ^2) tests (or Fisher's exact tests) and the student's *t*-tests (or Mann–Whitney U-tests) were applied appropriately to the univariable analysis of hemorrhagic growth. Multivariable logistic regression was performed to determine factors associated with three types of hemorrhagic growth (HE, IVHG, and RHE) by including factors showing *P* values ≤ 0.1 at the univariable analysis. The adjusted odds ratio (aOR) and 95% confidence intervals (CIs) were calculated.

The sensitivity, specificity, and positive predictive value (PPV) of the NCCT signs for the three types of hemorrhagic growth (HE, IVHG, and RHE) were also calculated and stratified according to OIT. All statistical tests reported two-sided *P* values, with $P < 0.05$ as the threshold for statistical significance. The R statistical software (version 4.0.3; https://www.r-project.org/) was used to perform all statistical analyses.

RESULTS

Study Population

Overall, 6141 patients were screened, of whom 1488 (mean age, 61 years; 65% male) were eligible (flowchart in Fig. 2). Of these ICHs, data were complete for all variables except mRS (missing data in 235 [16%]). The median OIT was 2.29 h (IQR, 1.42–3.55 h), and the follow-up NCCT time was 19.00 h (IQR, 9.89–33.04 h).

Quantitative data regarding the agreement of ICH volume measurements between the two researchers are available in the Supplement (Supplementary Tables 1-4 and Supplementary Figs. 1-4). The rate of NCCT signs ranged from 5.85% to 44.96%. There was substantial or excellent agreement between the observers for the identification of hypodensities (κ = 0.84), swirl sign (κ = 0.81), black hole sign (κ = 0.81), blend sign (κ = 0.85), fluid level (κ = 0.88), heterogeneous density (κ = 0.78), island sign (κ = 0.79), satellite sign (κ = 0.84), and irregular shape (κ = 0.78). The characteristics of the patients with and without imaging signs are summarized in Supplementary Tables 5-9.

Univariable Analysis of the Association with Hemorrhagic Growth (HE, IVHG, and RHE)

HE, IVHG, and RHE were observed in 418 (28%), 303 (20%), and 583 (39%) of 1488 patients, respectively. Of 583 cases with RHE, the proportion for hypodensities, swirl sign, black hole sign, blend sign, heterogeneous density, island sign, satellite sign, and irregular shape was 60%, 62%, 28%, 41%, 30%, 34%, 48%, and 43%, respectively. A

 https://doi.org/10.3348/kjr.2023.0591

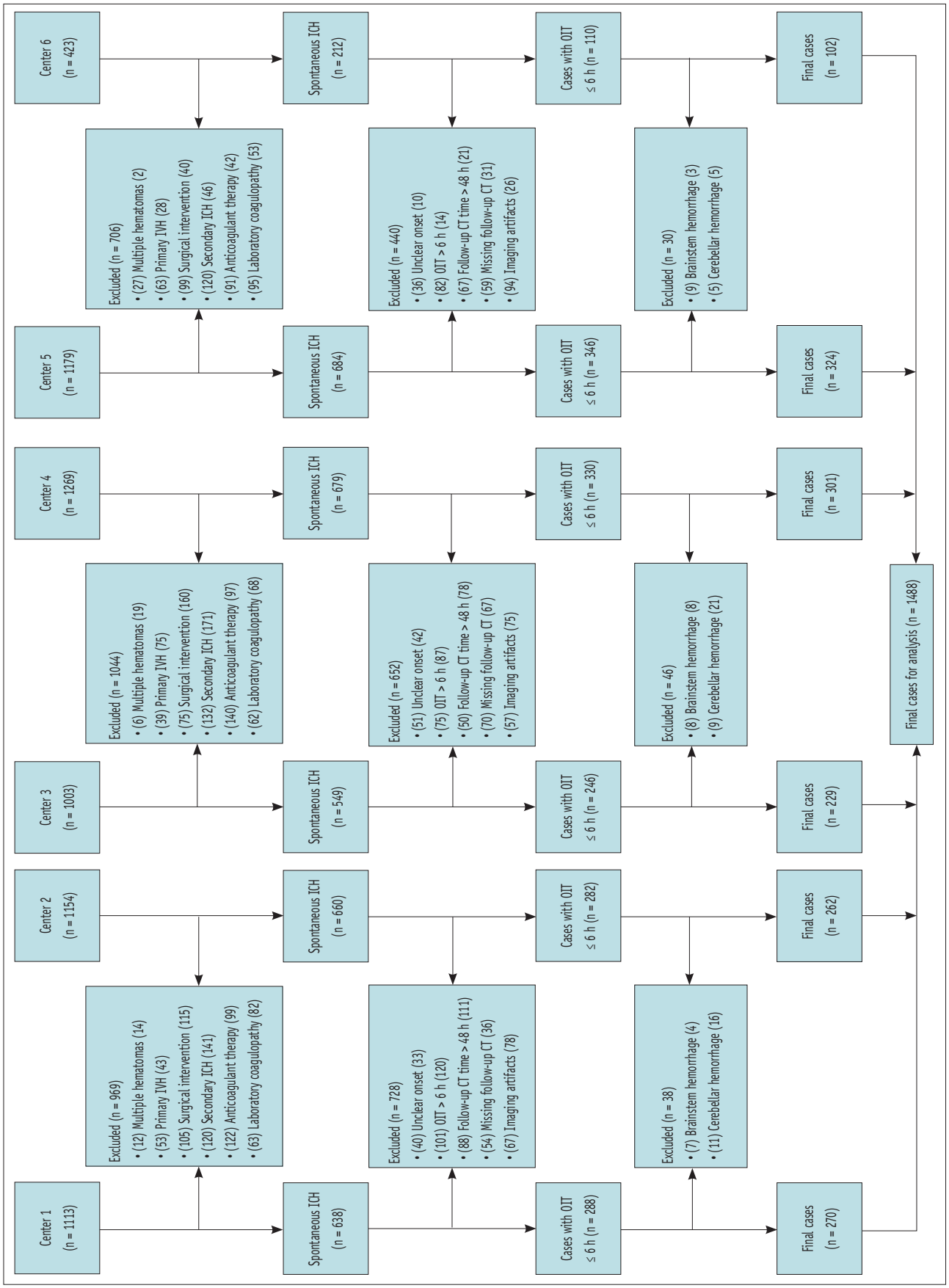

Fig. 2. Study inclusion and exclusion flowchart. ICH = intracerebral hemorrhage, OIT = onset-to-imaging time, IVH = intraventricular hemorrhage

https://doi.org/10.3348/kjr.2023.0591

Korean Journal of Radiology
KJR

Table 1. Univariable analysis for HE, IVHG, and RHE

	No HE (n = 1070)	HE (n = 418)	*P*	No IVHG (n = 1185)	IVHG (n = 303)	*P*	No RHE (n = 905)	RHE (n = 583)	*P*
Age, yr	62 ± 12	59 ± 12	< 0.001	61 ± 12	63 ± 13	0.001	61 ± 12	61 ± 13	0.344
Sex, male	668 (62)	294 (70)	0.004	767 (65)	195 (64)	0.904	569 (63)	393 (67)	0.074
Alcohol	290 (27)	114 (27)	0.947	325 (27)	79 (26)	0.636	249 (28)	155 (27)	0.695
Smoking	279 (26)	118 (28)	0.398	321 (27)	76 (25)	0.481	244 (27)	153 (26)	0.760
Medical history									
ICH	113 (11)	46 (11)	0.803	120 (10)	39 (13)	0.168	94 (10)	65 (11)	0.642
Cerebral infarct	141 (13)	51 (12)	0.614	156 (13)	36 (12)	0.552	119 (13)	73 (13)	0.724
Hypertension	746 (70)	295 (71)	0.747	846 (71)	195 (64)	0.017	642 (71)	399 (68)	0.304
Diabetes	109 (10)	42 (10)	0.936	120 (10)	31 (10)	0.957	92 (10)	59 (10)	0.977
Laboratory values									
Glucose, mmol/L	7.63 ± 3.07	7.64 ± 3.28	0.960	7.51 ± 3.08	8.10 ± 3.25	0.003	7.51 ± 3.00	7.82 ± 3.31	0.059
Platelet count, 10^9/L	200 ± 61	197 ± 68	0.309	200 ± 62	195 ± 66	0.226	201 ± 62	196 ± 65	0.149
INR	0.96 ± 0.10	0.97 ± 0.11	0.362	0.96 ± 0.10	0.98 ± 0.11	0.132	0.96 ± 0.10	0.97 ± 0.11	0.134
Clinical characteristics									
SBP, mmHg	168 ± 26	170 ± 29	0.103	167 ± 26	174 ± 29	< 0.001	167 ± 25	171 ± 28	0.007
DBP, mmHg	97 ± 17	99 ± 17	0.081	97 ± 17	99 ± 19	0.198	97 ± 17	98 ± 18	0.208
GCS score	12 (10–14)	10 (8–13)	< 0.001	13 (10–14)	10 (7–12)	< 0.001	13 (10–14)	10 (8–13)	< 0.001
OIT, h	2.58 (1.65–3.83)	1.70 (1.12–2.57)	< 0.001	2.47 (1.53–3.72)	1.77 (1.18–2.65)	< 0.001	2.69 (1.77–3.90)	1.75 (1.17–2.70)	< 0.001
Follow-up NCCT time, h	20.35 (11.00–36.00)	15.50 (6.62–26.50)	< 0.001	20.47 (10.49–37.63)	15.00 (6.50–24.50)	< 0.001	21.00 (11.00–40.00)	16.00 (7.52–26.50)	< 0.001
Radiographic features									
Baseline ICH volume, mL	10.73 (5.75–19.46)	16.73 (8.79–29.22)	< 0.001	11.04 (5.76–20.74)	15.34 (8.93–31.91)	< 0.001	10.13 (5.22–18.82)	15.47 (8.68–29.01)	< 0.001
Presence of IVH	373 (35)	90 (22)	< 0.001	274 (23)	189 (62)	< 0.001	242 (27)	221 (38)	< 0.001
ICH locations			< 0.001			< 0.001			0.036
Basal ganglia	537 (50)	246 (59)		671 (57)	112 (37)		495 (55)	288 (49)	
Thalamus	352 (33)	67 (16)		277 (23)	142 (47)		254 (28)	165 (28)	
Lobar	181 (17)	105 (25)		237 (20)	49 (16)		156 (17)	130 (22)	
Imaging signs									
Hypodensities	282 (26)	277 (66)	< 0.001	389 (33)	170 (56)	< 0.001	209 (23)	350 (60)	< 0.001
Swirl sign	388 (36)	281 (67)	< 0.001	494 (42)	175 (58)	< 0.001	306 (34)	363 (62)	< 0.001
Black hole sign	135 (13)	129 (31)	< 0.001	181 (15)	83 (27)	< 0.001	101 (11)	163 (28)	< 0.001
Blend sign	127 (12)	218 (52)	< 0.001	278 (23)	67 (22)	0.620	108 (12)	237 (41)	< 0.001
Fluid level	50 (5)	37 (9)	0.002	73 (6)	14 (5)	0.308	46 (5)	41 (7)	0.118
Heterogeneous density	174 (16)	144 (34)	< 0.001	228 (19)	90 (30)	< 0.001	142 (16)	176 (30)	< 0.001
Island sign	222 (21)	142 (34)	< 0.001	263 (22)	101 (33)	< 0.001	166 (18)	198 (34)	< 0.001
Satellite sign	399 (37)	200 (48)	< 0.001	456 (38)	143 (47)	0.006	319 (35)	280 (48)	< 0.001
Irregular shape	347 (32)	173 (41)	0.001	387 (33)	133 (44)	< 0.001	271 (30)	249 (43)	< 0.001
Outcome									
90-d mRS ≥ 3*	403 (46)	310 (81)	< 0.001	467 (48)	246 (90)	< 0.001	277 (38)	436 (83)	< 0.001

Values are expressed as mean ± standard deviation, n (%) or median (interquartile range).
*235/1488 (16%) missing values.
HE = hematoma expansion, IVHG = IVH growth, RHE = revised HE, ICH = intracerebral hemorrhage, INR = international normalized ratio, SBP = systolic blood pressure, DBP = diastolic blood pressure, GCS = Glasgow Coma Scale, OIT = onset-to-imaging time, NCCT = non-contrast CT, IVH = intraventricular hemorrhage, mRS = modified Rankin Scale

https://doi.org/10.3348/kjr.2023.0591

similar trend in other signs was found for IVHG, except for the blend sign and fluid level. Concomitantly, patients with any type of hemorrhagic growth (HE, IVHG, or RHE) had worse mRS scores at 90 days. A more detailed comparison between patients with and without hemorrhagic growth is presented in Table 1.

Table 2. Multivariable logistic regression for hematoma expansion

	Adjusted OR	95% CI	*P*
Hypodensities			
Absent	Reference category		
Present	7.99	4.87–13.40	< 0.001
Swirl sign			
Absent	Reference category		
Present	0.82	0.51–1.30	0.400
Black hole sign			
Absent	Reference category		
Present	1.25	0.83–1.90	0.286
Blend sign			
Absent	Reference category		
Present	10.60	7.36–15.30	< 0.001
Fluid level			
Absent	Reference category		
Present	0.95	0.52–1.72	0.871
Heterogeneous density			
Barras density scale < 3	Reference category		
Barras density scale ≥ 3	0.80	0.53–1.20	0.282
Island sign			
Absent	Reference category		
Present	2.75	1.64–4.67	< 0.001
Satellite sign			
Absent	Reference category		
Present	0.77	0.51–1.16	0.223
Irregular shape			
Barras shape scale < 3	Reference category		
Barras shape scale ≥ 3	0.69	0.43–1.11	0.131
Age (for 1 yr)	0.99	0.97–1.00	0.029
Sex			
Female	Reference category		
Male	1.38	1.00–1.91	0.051
DBP (for 1 mmHg)	1.00	0.99–1.01	0.848
GCS score (for increase by 1)	0.87	0.82–0.92	< 0.001
OIT (for 1 h)	0.59	0.52–0.66	< 0.001
Follow-up NCCT time (for 1 h)	0.99	0.98–1.00	0.177
Baseline ICH volume (for 1 mL)	0.99	0.98–1.00	0.193
IVH			
Absent	Reference category		
Present	0.54	0.36–0.82	0.004
ICH locations			
Basal ganglia	Reference category		
Thalamus	1.43	0.89–2.30	0.141
Lobar	1.23	0.81–1.87	0.338

OR = odds ratio, CI = confidence interval, DBP = diastolic blood pressure, GCS = Glasgow Coma Scale, OIT = onset-to-imaging time, NCCT = non-contrast CT, ICH = intracerebral hemorrhage, IVH = intraventricular hemorrhage

https://doi.org/10.3348/kjr.2023.0591

Korean Journal of Radiology
KJR

Multivariable Analysis of the Association with Hemorrhagic Growth (HE, IVHG, and RHE)

Regardless of which definition of hemorrhagic growth was applied, hypodensities were independent predictors of HE, IVHG, and RHE (aOR = 7.99 [95% CI = 4.87–13.40], aOR = 3.64 [95% CI = 2.15–6.24], and aOR = 7.90 [95% CI = 4.93–12.90], respectively), as was OIT. Both blend sign and island sign were associated with HE (aOR = 10.60 [95% CI = 7.36–15.30] and aOR = 2.75 [95% CI = 1.64–4.67]). The same was true for the blend sign and island sign on RHE (aOR = 10.10 [95% CI = 7.10–14.60] and aOR = 2.62 [95% CI = 1.60–4.30]). Additionally, heterogeneous density was also significantly associated with RHE (aOR = 0.61 [95% CI = 0.41–0.92]). The results are presented in Tables 2-4.

Performance of NCCT Signs for Hemorrhagic Growth Stratified by OIT

Table 5 summarizes the performance results. Of note, hypodensities had a poor predictive capacity for IVHG (PPV ≤ 0.41). The PPVs of most signs of RHE were higher than

Table 3. Multivariable logistic regression for IVH growth

	Adjusted OR	95% CI	*P*
Hypodensities			
Absent	Reference category		
Present	3.64	2.15–6.24	< 0.001
Swirl sign			
Absent	Reference category		
Present	0.73	0.44–1.21	0.226
Black hole sign			
Absent	Reference category		
Present	0.96	0.61–1.50	0.862
Heterogeneous density			
Barras density scale < 3	Reference category		
Barras density scale ≥ 3	0.95	0.62–1.46	0.832
Island sign			
Absent	Reference category		
Present	1.58	0.92–2.72	0.100
Satellite sign			
Absent	Reference category		
Present	1.01	0.66–1.53	0.979
Irregular shape			
Barras shape scale < 3	Reference category		
Barras shape scale ≥ 3	0.75	0.46–1.21	0.243
Age (for 1 yr)	1.01	1.00–1.02	0.130
Glucose (for 1 mmol/L)	1.00	0.95–1.05	0.942
SBP (for 1 mmHg)	1.01	1.00–1.01	0.029
GCS score (for increase by 1)	0.87	0.82–0.92	< 0.001
OIT (for 1 h)	0.72	0.64–0.81	< 0.001
Follow-up NCCT time (for 1 h)	0.99	0.98–1.00	0.011
Baseline ICH volume (for 1 mL)	1.03	1.02–1.05	< 0.001
IVH			
Absent	Reference category		
Present	2.89	2.01–4.17	< 0.001
ICH locations			
Basal ganglia	Reference category		
Thalamus	3.93	2.48–6.26	< 0.001
Lobar	0.57	0.34–0.93	0.027

IVH = intraventricular hemorrhage, OR = odds ratio, CI = confidence interval, SBP = systolic blood pressure, GCS = Glasgow Coma Scale, OIT = onset-to-imaging time, NCCT = non-contrast CT, ICH = intracerebral hemorrhage

https://doi.org/10.3348/kjr.2023.0591

Table 4. Multivariable logistic regression for revised hematoma expansion

	Adjusted OR	95% CI	*P*
Hypodensities			
Absent	Reference category		
Present	7.90	4.93–12.90	< 0.001
Swirl sign			
Absent	Reference category		
Present	0.88	0.57–1.35	0.573
Black hole sign			
Absent	Reference category		
Present	1.12	0.73–1.72	0.591
Blend sign			
Absent	Reference category		
Present	10.10	7.10–14.60	< 0.001
Heterogeneous density			
Barras density scale < 3	Reference category		
Barras density scale ≥ 3	0.61	0.41–0.92	0.017
Island sign			
Absent	Reference category		
Present	2.62	1.60–4.30	< 0.001
Satellite sign			
Absent	Reference category		
Present	0.88	0.61–1.28	0.514
Irregular shape			
Barras shape scale < 3	Reference category		
Barras shape scale ≥ 3	0.78	0.50–1.20	0.257
Sex			
Female	Reference category		
Male	1.22	0.91–1.64	0.175
Glucose (for 1 mmol/L)	1.00	0.96–1.05	0.817
SBP (for 1 mmHg)	1.00	1.00–1.01	0.747
GCS score (for increase by 1)	0.87	0.83–0.91	< 0.001
OIT (for 1 h)	0.61	0.54–0.67	< 0.001
Follow-up NCCT time (for 1 h)	0.99	0.98–1.00	0.070
Baseline ICH volume (for 1 mL)	1.01	1.00–1.02	0.195
IVH			
Absent	Reference category		
Present	1.89	1.32–2.72	< 0.001
ICH locations			
Basal ganglia	Reference category		
Thalamus	2.95	1.94–4.51	< 0.001
Lobar	0.99	0.66–1.48	0.945

OR = odds ratio, CI = confidence interval, SBP = systolic blood pressure, GCS = Glasgow Coma Scale, OIT = onset-to-imaging time, NCCT = non-contrast CT, ICH = intracerebral hemorrhage, IVH = intraventricular hemorrhage

those of HE. Hypodensities, blend sign, and island sign showed high PPVs ≥ 0.80 when OIT was ≤ 2 h. The highest PPV for HE was observed with the blend sign when OIT was ≤ 2 h (0.84).

DISCUSSION

In this study, we comprehensively investigated the potential role of NCCT in the growth of three ICH types. Hypodensities, blend sign, and island sign were independent predictors of the HE and RHE. We also tested

https://doi.org/10.3348/kjr.2023.0591

Korean Journal of Radiology
KJR

Table 5. Performance of NCCT signs for hemorrhagic growth stratified by OIT

	HE			IVH growth			RHE		
	Sensitivity	Specificity	PPV	Sensitivity	Specificity	PPV	Sensitivity	Specificity	PPV
Hypodensities									
≤ 2 h	0.67 (175/261)	0.74 (265/359)	0.65 (175/269)	0.63 (110/176)	0.64 (285/444)	0.41 (110/269)	0.62 (215/346)	0.80 (220/274)	0.80 (215/269)
2–4 h	0.65 (81/125)	0.74 (362/487)	0.39 (81/206)	0.49 (48/97)	0.69 (357/515)	0.23 (48/206)	0.59 (106/181)	0.77 (331/431)	0.51 (106/206)
4–6 h	0.66 (21/32)	0.72 (161/224)	0.25 (21/84)	0.40 (12/30)	0.68 (154/226)	0.14 (12/84)	0.52 (29/56)	0.73 (145/200)	0.35 (29/84)
≤ 6 h	0.66 (277/418)	0.74 (788/1070)	0.50 (277/559)	0.56 (170/303)	0.67 (796/1185)	0.30 (170/559)	0.60 (350/583)	0.77 (696/905)	0.63 (350/559)
Blend sign									
≤ 2 h	0.51 (132/261)	0.93 (334/359)	0.84 (132/157)	-	-	-	0.41 (142/346)	0.95 (259/274)	0.90 (142/157)
2–4 h	0.56 (70/125)	0.86 (418/487)	0.50 (70/139)	-	-	-	0.40 (73/181)	0.85 (365/431)	0.53 (73/139)
4–6 h	0.50 (16/32)	0.85 (191/224)	0.33 (16/49)	-	-	-	0.39 (22/56)	0.87 (173/200)	0.45 (22/49)
≤ 6 h	0.52 (218/418)	0.88 (943/1070)	0.63 (218/345)	-	-	-	0.41 (237/583)	0.88 (797/905)	0.69 (237/345)
Heterogeneous density									
≤ 2 h	-	-	-	-	-	-	0.32 (111/346)	0.85 (234/274)	0.74 (111/151)
2–4 h	-	-	-	-	-	-	0.28 (50/181)	0.85 (365/431)	0.43 (50/116)
4-6 h	-	-	-	-	-	-	0.27 (15/56)	0.82 (164/200)	0.29 (15/51)
≤ 6 h	-	-	-	-	-	-	0.30 (176/583)	0.84 (763/905)	0.55 (176/318)
Island sign									
≤ 2 h	0.30 (78/261)	0.87 (313/359)	0.63 (78/124)	-	-	-	0.30 (103/346)	0.92 (253/274)	0.83 (103/124)
2–4 h	0.41 (51/125)	0.75 (366/487)	0.30 (51/172)	-	-	-	0.40 (73/181)	0.77 (332/431)	0.42 (73/172)
4–6 h	0.41 (13/32)	0.75 (169/224)	0.19 (13/68)	-	-	-	0.39 (22/56)	0.77 (154/200)	0.32 (22/68)
≤ 6 h	0.34 (142/418)	0.79 (848/1070)	0.39 (142/364)	-	-	-	0.34 (198/583)	0.82 (739/905)	0.54 (198/364)

The numbers of patients within ≤ 2 h, 2–4 h, 4–6 h, and ≤ 6 h were 620, 612, 256, and 1488, respectively.
NCCT = non-contrast CT, OIT = onset-to-imaging time, HE = hematoma expansion, IVH = intraventricular hemorrhage, RHE = revised HE, PPV = positive predictive value

the performance of the above-mentioned three signs in the prediction of hemorrhagic growth, and the PPV for each sign on RHE was greater than 0.80 within 2 h.

Previous studies demonstrated that IVHG was strongly associated with patient outcomes after ICH [7,8,10]. Patients with ICH without high-risk HE, but with IVHG, if present, are not generally considered to have poor outcomes according to the conventional definition of HE [6]. This may have resulted in an underestimation of the risk of neurological deterioration. Our findings confirmed that patients in the RHE group had a more adverse prognosis, suggesting that the definition of RHE reflects the outcome more accurately than HE or IVHG alone after ICH. As an alternative, NCCT signs have been the major focus of HE

 https://doi.org/10.3348/kjr.2023.0591

prediction, but their role in RHE has been relatively spared [17-23]. Notably, obvious overlaps exist among different signs, leading to heterogeneity in findings [11]. Therefore, a comprehensive evaluation of RHE signs is necessary.

This study measured the predictive ability of hemorrhagic growth signs after stratification based on the OIT. The sooner the signs are identified, the more accurate the prediction. This suggests that these signs have a time-dependent effect on hemorrhagic growth. In patients with ICH within 2 h of onset, the PPVs of the signs of hemorrhagic growth were significantly higher than those in patients with an onset time > 2 h, particularly for the prediction of hypodensities, blend sign, and island sign on RHE. Similar to our study, Morotti et al. [14] reported a PPV of 0.43 for hypodensities in predicting HE within 2 h in patients with ICH. The latest results from a Mobile Stroke Unit Study found that HE was more frequent in the first 2 h, with 28% occurring within the first h after onset and 17% occurring within 1–2 h after onset [24]. The present study supplements the aforementioned studies. In ICH, early comprehensive care is important because some treatments are more effective when applied [2-4]. Hemostatic therapy is more appropriate for patients at high risk of ICH growth [25]. Thus, capturing earlier signs may considerably identify patients at high risk for RHE, which could result in an improved prognosis.

It is well established that overlap inevitably exists among NCCT signs [11]. This could have contributed to the heterogeneity among the studies. Nevertheless, our results confirmed that hypodensities, blend sign, and island sign were independent of each other and positively correlated with RHE. These compounds have extremely high potential for clinical applications. Various other technologies have also been used to predict hemorrhagic growth [26,27]. The performance of the radiomics model proposed by Xia et al. [26] was significantly better than the NCCT signs obtained in our study. The advantage of radiomics lies in the quantitative analysis of image features that do not rely on subjective judgment [28]. However, radiomics analysis is limited by the repeatability and reproducibility of radiomics features, which is not conducive to large-scale promotion and application in clinical practice [29,30]. Furthermore, artificial intelligence-assisted diagnosis and prediction of the disease has made significant progress in recent years [27,31]. Ma et al. [27] developed an end-to-end deep learning method to automatically segment hematomas for HE prediction, with ResNet-34 achieving an excellent area under the curve (0.9267). This technique appears promising for HE prediction, but it remains largely unknown whether it is also effective for predicting RHE and requires further investigation in the future. Although the performance of conventional NCCT signs is inferior to that of the above technologies, these indicators have convenient and rapid characteristics in clinical practice as favorable prognostic predictors [11,19,32], especially in emergency settings or primary health institutions [33-35].

The strengths and limitations of this study are as follows. Its strengths include the recruitment of a cohort of representative and diverse patients with ICH from six centers and the relatively large number of cases of hemorrhagic growth at 2 h of ictus onset. However, retrospective observational studies are subject to limitations inherent to the methodology. First, the follow-up NCCT time was based on clinical decisions, which may have underestimated the prevalence and lowered the detection of hemorrhagic growth. Second, the incidence and risk profiles of ICH among different hospitals might have resulted in a selection bias. This factor also significantly increases the chances of targeted surgical interventions at senior stroke centers being provided earlier than necessary, particularly in patients with a larger hematoma volume or intraparenchymal hematoma with IVH. Third, the evaluation of NCCT signs relies on visual inspection, and potential interference may arise from image noise. Judging the signs of a small hematoma is also particularly challenging when facing the current spatial resolution of imaging equipment in different centers. Finally, patients without 90-day follow-up mRS scores were excluded. Therefore, the associations between NCCT signs and mRS scores were not analyzed further.

In conclusion, this study demonstrated an association between NCCT signs and hemorrhagic growth (HE, IVHG, and RHE) after ICH. Hypodensities, blend sign, and island sign were the best NCCT predictors of RHE when OIT was ≤ 2 h. NCCT signs may assist in earlier recognition of the risk of hemorrhagic growth and guide early intervention to prevent neurological deterioration from hemorrhagic growth.

Supplement

The Supplement is available with this article at https://doi.org/10.3348/kjr.2023.0591.

Availability of Data and Material

The datasets generated or analyzed during the study are

Korean Journal of Radiology
KJR

available from the corresponding author on reasonable request.

Conflicts of Interest

The authors have no potential conflicts of interest to disclose.

Author Contributions

Conceptualization: Lei Song. Data curation: Lei Song, Yongqiang Yu, Tingting Guo. Formal analysis: Tingting Guo. Funding acquisition: Yongqiang Yu. Investigation: Lei Song, Yongqiang Yu, Tingting Guo. Methodology: Lei Song, Cun Zhang, Ji Zhang. Project administration: Yongqiang Yu, Xiaoming Qiu, Longsheng Wang. Resources: Lei Song, Hang Zhou, Wenmin Guo, Yu Ye, Rujia Wang, Liwei Zou. Software: Hang Zhou, Yu Ye, Dongfang Tang. Supervision: Yongqiang Yu, Tingting Guo, Longsheng Wang. Validation: Hang Zhou, Wenmin Guo, Yu Ye. Visualization: Tingting Guo, Cun Zhang. Writing—original draft: Lei Song. Writing—review & editing: all authors.

ORCID IDs

Lei Song
https://orcid.org/0000-0001-8975-5060
Xiaoming Qiu
https://orcid.org/0009-0002-6579-4860
Cun Zhang
https://orcid.org/0000-0002-7585-1593
Hang Zhou
https://orcid.org/0009-0004-1945-7868
Wenmin Guo
https://orcid.org/0009-0008-0598-632X
Yu Ye
https://orcid.org/0000-0001-8953-249X
Rujia Wang
https://orcid.org/0000-0003-2424-6569
Hui Xiong
https://orcid.org/0009-0004-9368-6319
Ji Zhang
https://orcid.org/0009-0007-7883-6018
Dongfang Tang
https://orcid.org/0009-0006-6960-4736
Liwei Zou
https://orcid.org/0000-0003-0316-2876
Longsheng Wang
https://orcid.org/0000-0002-3791-8486
Yongqiang Yu
https://orcid.org/0000-0001-8977-2215
Tingting Guo
https://orcid.org/0009-0006-8743-8890

Funding Statement

This work was supported by the National Natural Science Foundation of China (grant number 81771817, 81801679, 82071905).

Acknowledgments

We appreciate the statistical consultation and analyses of Cun Zhang, The First Affiliated Hospital of University of Science and Technology of China. We would also like to thank Editage (www.editage.cn) for English language editing.

REFERENCES

1. GBD 2019 Diseases and Injuries Collaborators. Global burden of 369 diseases and injuries in 204 countries and territories, 1990-2019: a systematic analysis for the global burden of disease study 2019. *Lancet* 2020;396:1204-1222
2. Sheth KN. Spontaneous intracerebral hemorrhage. *N Engl J Med* 2022;387:1589-1596
3. Greenberg SM, Ziai WC, Cordonnier C, Dowlatshahi D, Francis B, Goldstein JN, et al. 2022 guideline for the management of patients with spontaneous intracerebral hemorrhage: a guideline from the American Heart Association/American Stroke Association. *Stroke* 2022;53:e282-e361
4. Morotti A, Boulouis G, Dowlatshahi D, Li Q, Shamy M, Al-Shahi Salman R, et al. Intracerebral haemorrhage expansion: definitions, predictors, and prevention. *Lancet Neurol* 2023;22:159-171
5. Sprigg N, Flaherty K, Appleton JP, Al-Shahi Salman R, Bereczki D, Beridze M, et al. Tranexamic acid for hyperacute primary IntraCerebral Haemorrhage (TICH-2): an international randomised, placebo-controlled, phase 3 superiority trial. *Lancet* 2018;391:2107-2115
6. Yogendrakumar V, Moores M, Sikora L, Shamy M, Ramsay T, Fergusson D, et al. Evaluating hematoma expansion scores in acute spontaneous intracerebral hemorrhage: a systematic scoping review. *Stroke* 2020;51:1305-1308
7. Yogendrakumar V, Ramsay T, Fergusson D, Demchuk AM, Aviv RI, Rodriguez-Luna D, et al. New and expanding ventricular hemorrhage predicts poor outcome in acute intracerebral hemorrhage. *Neurology* 2019;93:e879-e888
8. Li Q, Li R, Zhao LB, Yang XM, Yang WS, Deng L, et al. Intraventricular hemorrhage growth: definition, prevalence and association with hematoma expansion and prognosis. *Neurocrit Care* 2020;33:732-739
9. Yogendrakumar V, Ramsay T, Fergusson DA, Demchuk AM, Aviv RI, Rodriguez-Luna D, et al. Redefining hematoma expansion with the inclusion of intraventricular hemorrhage growth.

Stroke 2020;51:1120-1127
10. Yang WS, Zhang SQ, Shen YQ, Wei X, Zhao LB, Xie XF, et al. Noncontrast computed tomography markers as predictors of revised hematoma expansion in acute intracerebral hemorrhage. *J Am Heart Assoc* 2021;10:e018248
11. Morotti A, Boulouis G, Dowlatshahi D, Li Q, Barras CD, Delcourt C, et al. Standards for detecting, interpreting, and reporting noncontrast computed tomographic markers of intracerebral hemorrhage expansion. *Ann Neurol* 2019;86:480-492
12. Law ZK, Ali A, Krishnan K, Bischoff A, Appleton JP, Scutt P, et al. Noncontrast computed tomography signs as predictors of hematoma expansion, clinical outcome, and response to tranexamic acid in acute intracerebral hemorrhage. *Stroke* 2020;51:121-128
13. Al-Shahi Salman R, Frantzias J, Lee RJ, Lyden PD, Battey TWK, Ayres AM, et al. Absolute risk and predictors of the growth of acute spontaneous intracerebral haemorrhage: a systematic review and meta-analysis of individual patient data. *Lancet Neurol* 2018;17:885-894
14. Morotti A, Li Q, Mazzoleni V, Nawabi J, Schlunk F, Mazzacane F, et al. Non-contrast CT markers of intracerebral hemorrhage expansion: the influence of onset-to-CT time. *Int J Stroke* 2023;18:704-711
15. Dowlatshahi D, Brouwers HB, Demchuk AM, Hill MD, Aviv RI, Ufholz LA, et al. Predicting intracerebral hemorrhage growth with the spot sign: the effect of onset-to-scan time. *Stroke* 2016;47:695-700
16. Falcone GJ, Biffi A, Brouwers HB, Anderson CD, Battey TW, Ayres AM, et al. Predictors of hematoma volume in deep and lobar supratentorial intracerebral hemorrhage. *JAMA Neurol* 2013;70:988-994
17. Leasure AC, Sheth KN, Comeau M, Aldridge C, Worrall BB, Vashkevich A, et al. Identification and validation of hematoma volume cutoffs in spontaneous, supratentorial deep intracerebral hemorrhage. *Stroke* 2019;50:2044-2049
18. Dowlatshahi D, Demchuk AM, Flaherty ML, Ali M, Lyden PL, Smith EE; VISTA Collaboration. Defining hematoma expansion in intracerebral hemorrhage: relationship with patient outcomes. *Neurology* 2011;76:1238-1244
19. Wartenberg KE. Attacking intracerebral hemorrhage expansion: noncontrast CT markers on the horizon. *Neurology* 2020;95:615-616
20. Cai J, Zhu H, Yang D, Yang R, Zhao X, Zhou J, et al. Accuracy of imaging markers on noncontrast computed tomography in predicting intracerebral hemorrhage expansion. *Neurol Res* 2020;42:973-979
21. Quintas-Neves M, Marques L, Silva L, Amorim JM, Ferreira C, Pinho J. Noncontrast computed tomography markers of outcome in intracerebral hemorrhage patients. *Neurol Res* 2019;41:1083-1089
22. Kim YS, Chae HY, Jeong HG, Kim BJ, Lee SU, Kang J, et al. Size-related differences in computed tomography markers of hematoma expansion in acute intracerebral hemorrhage. *Neurocrit Care* 2022;36:602-611
23. Morotti A, Arba F, Boulouis G, Charidimou A. Noncontrast CT markers of intracerebral hemorrhage expansion and poor outcome: a meta-analysis. *Neurology* 2020;95:632-643
24. Bowry R, Parker SA, Bratina P, Singh N, Yamal JM, Rajan SS, et al. Hemorrhage enlargement is more frequent in the first 2 hours: a prehospital mobile stroke unit study. *Stroke* 2022;53:2352-2360
25. Nie X, Liu J, Liu D, Zhou Q, Duan W, Pu Y, et al. Haemostatic therapy in spontaneous intracerebral haemorrhage patients with high-risk of haematoma expansion by CT marker: a systematic review and meta-analysis of randomised trials. *Stroke Vasc Neurol* 2021;6:170-179
26. Xia X, Ren Q, Cui J, Dong H, Huang Z, Jiang Q, et al. Radiomics for predicting revised hematoma expansion with the inclusion of intraventricular hemorrhage growth in patients with supratentorial spontaneous intraparenchymal hematomas. *Ann Transl Med* 2022;10:8
27. Ma C, Wang L, Gao C, Liu D, Yang K, Meng Z, et al. Automatic and efficient prediction of hematoma expansion in patients with hypertensive intracerebral hemorrhage using deep learning based on CT images. *J Pers Med* 2022;12:779
28. Lambin P, Leijenaar RTH, Deist TM, Peerlings J, de Jong EEC, van Timmeren J, et al. Radiomics: the bridge between medical imaging and personalized medicine. *Nat Rev Clin Oncol* 2017;14:749-762
29. Zwanenburg A, Vallières M, Abdalah MA, Aerts HJWL, Andrearczyk V, Apte A, et al. The image biomarker standardization initiative: standardized quantitative radiomics for high-throughput image-based phenotyping. *Radiology* 2020;295:328-338
30. Berenguer R, Pastor-Juan MDR, Canales-Vázquez J, Castro-García M, Villas MV, Mansilla Legorburo F, et al. Radiomics of CT features may be nonreproducible and redundant: influence of CT acquisition parameters. *Radiology* 2018;288:407-415
31. Cellina M, Cè M, Irmici G, Ascenti V, Caloro E, Bianchi L, et al. Artificial intelligence in emergency radiology: where are we going? *Diagnostics (Basel)* 2022;12:3223
32. Nehme A, Ducroux C, Panzini MA, Bard C, Bereznyakova O, Boisseau W, et al. Non-contrast CT markers of intracerebral hematoma expansion: a reliability study. *Eur Radiol* 2022;32:6126-6135
33. Jain A, Malhotra A, Payabvash S. Imaging of spontaneous intracerebral hemorrhage. *Neuroimaging Clin N Am* 2021;31:193-203
34. Szentes T, Kovács L, Óváry C. New hospital structure in the twenty-first century: the position of level III (tertiary) neurological and stroke care in a changing healthcare system. *Springerplus* 2016;5:2039
35. Wang X, Birch S, Zhu W, Ma H, Embrett M, Meng Q. Coordination of care in the Chinese health care systems: a gap analysis of service delivery from a provider perspective. *BMC Health Serv Res* 2016;16:571

https://doi.org/10.3348/kjr.2023.0591